Ionics
https://doi.org/10.1007/s11581-018-2500-z

ORIGINAL PAPERS

A study on blend polymer electrolyte based on poly(vinyl alcohol)-poly (acrylonitrile) with magnesium nitrate for magnesium battery

R. Manjuladevi[1,2] · S. Selvasekarapandian[2,3] · M. Thamilselvan[4] · R. Mangalam[5] · S. Monisha[3,6] · P. Christopher Selvin[3]

Received: 15 January 2018 / Accepted: 14 February 2018

Abstract

Studies on magnesium ion conducting blend polymer electrolyte (BPE) at room temperature are reported. BPE films of optimized 92.5PVA:7.5PAN ratio in view of its maximum conductivity with various concentrations of magnesium salt—$Mg(NO_3)_2$—of different molar mass percentages (0.1, 0.2, 0.3, and 0.4 m.m.%) have been prepared using solution-casting technique with dimethylformamide (DMF) as solvent. The promising characteristic features of these films have been studied. Possible conformational changes in the polymer host 92.5PVA:7.5PAN due to $Mg(NO_3)_2$ entrapment have been investigated by FTIR and XRD analysis. The composition 92.5PVA:7.5PAN:0.3 m.m.% $Mg(NO_3)_2$ offers maximum electrical conductivity of 1.71×10^{-3} S/cm at room temperature. The σ values follow the Arrhenius equation, and the activation energy for the optimized composition is 0.36 eV. The variations in glass transition temperature have been found using differential scanning calorimeter. Mg^{2+} ion conduction in the BPE film is confirmed using transference number measurement and cyclic voltammetry. The transport number of the Mg^{2+} ion is 0.30. Using linear sweep voltammetry, the electrochemical stability window for the highest BPE has been measured. Primary magnesium battery has been constructed using the maximum conducting membrane, and its output characteristics have been studied.

Keywords Blend polymer electrolyte · Polyacrylonitrile · Magnesium nitrate · Ionic conductivity · Magnesium battery

Introduction

Due to the remarkable progress of energy storage systems, rechargeable power sources from sustainable assets with smart energy environment having significant electrochemical properties of high safeties are highly required [1]. Among different power sources, lithium ion batteries based on solid polymer electrolytes have many benefits which can enhance the safety and stability of batteries due to their non-leakage and non-reactive characteristics. Even though it is unrivaled in its act, there are extra worries such as high cost, low energy and power density, and highly explosive. The formation of dendrite during cycling in lithium batteries causes a mortal short circuit [2]. Therefore, it is aspired to develop a new type of green and safer, less expensive, non-dendrite rechargeable battery system. Owing to the intrinsic advantage of Mg metal, magnesium (Mg) battery has been turned up as an attractive alternate for next rank batteries. Magnesium can be electro-deposited efficiently without any dendrite growth [3], and it can also provide a higher theoretical volumetric capacity (3832 $mAhcm^{-3}$) due to the divalent atmosphere of Mg^{2+} than Li (2062 $mAhcm^{-3}$). This makes the Mg battery more spirited for energy storage devices [4]. In the Earth's crust, Mg is more abundant and more widely available than Li. The preparation of electrode with oxygen-rich environment is feasible with Mg metal. These merits make the door opened for magnesium batteries for next-generation energy storage.

✉ M. Thamilselvan
mthamil@rediffmail.com

[1] Department of Physics, SNS College of Engineering, Coimbatore, Tamil Nadu, India

[2] Materials Research Center, Coimbatore, Tamil Nadu, India

[3] Department of Physics, Bharathiar University, Coimbatore, Tamil Nadu, India

[4] Department of Physics, Thanthai Periyar Government Institute of Technology, Vellore, Tamil Nadu, India

[5] Department of Physics, PSG Institute of Technology and Applied Research, Coimbatore, Tamil Nadu, India

[6] Department of Physics, N.M.S.S. Vellaichamy Nadar College, Madurai, Tamil Nadu, India

Published online: 19 March 2018

In working state of a battery, the solid polymer electrolyte (SPE) plays as the separator for the electrodes in open state and also in the ion conductor medium between the electrodes. SPEs have been broadly studied for the past two decades due to their potential applications such as suitable for flexible type, leak proof and light weight, novel materials for the construction of ion conducting devices [5]. For the preparation of SPEs, the synthetic polar polymers namely poly(ethylene oxide) (PEO), poly(methylmethacrylate) (PMMA), poly(vinyl alcohol) (PVA), poly(acrylonitrile) (PAN), and poly(vinyl pyrrolidone) (PVP) are commonly used as host matrix for the preparation of SPEs. Habitually, the conduction mechanism of polymer electrolytes is based on the transport of the metal ion which is closely fixed to the polymer chains. The ionic transport of SPE occurs only in the amorphous polymer regions than in crystalline region and is often ruled by the segmental motion of the polymer chain [6]. The SPE forms the complexes of polymer with the ions of the added salt which have high amorphicity. The low ionic conductivity at ambient temperature limits the SPEs for numerous technological applications in which the vibrations of polymer chains are critical for the ion transportation. The ionic conductivity of the SPE can be increased by various approaches such as (i) use of conventional plasticizers like EC, PC, and DEC, (ii) dispersion of inorganic filler like SiO_2, Al_2O_3, CNT, and TiO_2, (iii) copolymerization, and (iv) blending. Among different approaches, concerning with the ample variety of application prospects, polymer blending technique has been utilized for developing and designing new polymeric materials [7]. The two main advantages of polymer blending are (i) appropriate control of physical properties by compositional changes and (ii) simplification of synthesis conditions. Later, Hema et al. synthesized a single Li-ion polymer for polyvinyl alcohol (PVA) which was blended with PVdF and $LiCF_3SO_3$ and TiO_2 as nanofiller to form Li-ion electrolyte with conductivity as high as 3.7×10^{-3} S cm^{-1} at room temperature [8]. When compared to pure PVA (2×10^{-10} S cm^{-1}), the PVA/PAN blend polymer electrolyte (BPE) with 3M $LiClO_4$ was noted to have an improved conductivity of 3.76×10^{-3} S cm^{-1} [9]. Anji et al. has recorded that the polymer electrolyte having 30 wt% of $Mg(NO_3)_2$ with PVA–PVP polymer blend has high ionic conductivity of 3.44×10^{-5} S/cm [10]. Further to achieve better conductivity, many blend electrolytes have been reported based on PVC/PEO [11], PVA/PMMA [12], PVdFHFP/PAN [13], and so on. Among various polymers, PVA is a biodegradable, biocompatible, and non-toxic inexpensive synthetic polymer with admirable film-forming properties. In aqueous blending PVA with long range, hydrogen bond-forming capacity results into better complex formation with enhanced physical and chemical properties. The preparation and characterization of PVA-based BPE membranes were assessed for the battery applications [14, 15]. By using various crystallization conditions and the blend component ratios composed by PVA and other crystalline polymers, can alter the crystalline structure of the blend. In this order, PAN is a suitable candidate to create a blend with PVA. PAN is a semicrystalline, synthetic resin prepared by the polymerization of acrylonitrile. PAN is a special conjugate polymer which can allow faster ionic mobility, and it is easily soluble in DMF. Hai-Kuan Yuan et al. investigated about the dehydration of ethyl acetate solution by means of pervaporation using PVA/PAN hollow fiber composite membrane [16]. The cause of the reaction of epichlorohydrin with hydrolyzed starch-g-PAN (HSPAN)/PVA blend films has been noted by Dae Hyun Kim et al. [17]. Xiao-Hua Maa et al. [18] analyzed the preparation and characterization of PFSA–PVA–SiO2/PVA/PAN difunctional hollow fiber composite membranes. When PVA and PAN are mixed, the interactions between them were likely to occur through interchain hydrogen bonding. PVA–PAN having good charge storage capacity and their electrical and optical properties prove it to be a good potential material when added with salt [19]. It has been optimized that the system comprising 92.5PVA:7.5PAN has the highest conductivity 1.2 × 10–7 S cm^{-1} [20]. Based on ammonium and lithium salts, there have been a few studies on this optimized blend composition [19, 21–23]. Literature survey reveals that only very small attention has been given to the polymer electrolytes based on PVA–PAN blend in which multivalent cations are the mobile species. Girish Kumar and Munichandraiah [24, 25] have effectively constructed working magnesium cells for the gel polymer electrolytes and manganese oxide (MnO_2) as cathode by using poly(vinylidenefluoride) (PVDF) and poly(methylmethacrylate) (PMMA) as polymer hosts. Osman et al. have recorded that 15% $Mg(ClO_4)_2$ and 20% $Mg(CF_3SO_3)_2$ can coordinate with PMMA gel polymer electrolyte system to give the maximum ionic conductivity of 3.31×10^{-3} and 1.27×10^{-3} S cm^{-1}, respectively [26]. The primary focus of the present investigation was to explore the impact of $Mg(NO_3)_2$ salt concentration on the structural, electrical, and optical properties of 92.5PVA:7.5PAN BPE film.

Experimental technique

In the present study, PVA with an average molecular weight of 1,25,000 from SD Fine-Chem Ltd. and PAN with an average molecular weight of 1,50,000 from Sigma-Aldrich have been used as starting material with magnesium nitrate ($Mg(NO_3)_2$) of molecular weight 256.41 g/mol from Hi-Media as salt. All were used without any further purification to prepare the blend polymer electrolytes. Dimethylformamide (DMF) with molecular weight 73.08 g/mol, density = 0.948–0.949 kg/m^3 from Merck specialties private Ltd., has been used as solvent.

Different molar mass ratios of 92.5PVA:7.5PAN:x $Mg(NO_3)_2$ where x = 0.1, 0.2, 0.3, and 0.4 have been prepared by solution-casting technique. In this technique, optimized

ratios of 92.5PVA and 7.5PAN have been dissolved individually in DMF, and these solutions have been mixed together and stirred well by using magnetic stirrer to obtain homogeneous mixture. Salts of different compositions (0.1, 0.2, 0.3, and 0.4 m.m.% $Mg(NO_3)_2$) have been separately dissolved in DMF, and it is mixed together with the blend polymer and allowed to stirred for 10 h. The obtained mixture is casted in petri dishes and is subjected for drying (60 °C for 2 days) in a vacuum oven. After drying, the transparent flexible films of thickness ranging from 150 to 200 μm were obtained. The obtained films were taken for further characterization.

Using CuKα radiation, X-ray diffraction (XRD) patterns have been recorded at room temperature on Philips X'PERT-PRO diffractometer in the range of 2θ=10°–80°. FTIR spectrum has been recorded for samples using ALPHA BRUKER FT-IR spectrophotometer in the wavenumber range 3000–800 cm^{-1} at room temperature with the resolution of 1 cm^{-1}. Using HIOKI 3532–50 LCR HITESTER, the impedance measurements have been carried out from room temperature to 343 K in the frequency range of 42 Hz to 1 MHz. BPEs of uniform thickness having an area of 1 cm^2 have been placed in between two stainless steel plates which act as blocking electrodes.. Glass transition temperature analysis of the samples has been studied using a differential scanning calorimeter (DSC) (Perkin Elmer DSC 4000 apparatus) by heating the samples from 20 to 200 °C in N_2 atmosphere at a heating rate of 20 °C/min. The transference number measurements have been calculated using Evans et al.'s polarization technique. Linear sweep voltammetry has been used to measure the working potential of the BPE. Primary magnesium battery using the membrane with the highest ionic conductivity as electrolyte has been constructed. The open-circuit voltage and discharge characteristics have been reported.

X-ray diffraction (XRD) analysis

The crystalline nature of polymer electrolyte can be studied by using XRD pattern analysis. The XRD diffraction patterns of pure polymer blend 92.5PVA:7.5PAN and salt-added polymer blend (92.5PVA:7.5PAN:x m.m.% $Mg(NO_3)_2$/x = 0.2, 0.3, and 0.4) have been shown in Fig. 1. Normally, a sharp peak with high intensity corresponds to semicrystalline materials and a broad peak corresponds to an amorphous material [27]. In Fig. 1, the two peaks one at about 20.3° with high intensity and another at about 40.8° with less intensity were clearly noted in the diffractograms of pure BPE (92.5PVA:7.5PAN) with high PVA content. These observed peak intensities which correspond to the PVA crystalline phase [19] decrease dramatically, and a broad hump was observed in the diffraction pattern of the BPE 92.5PVA:7.5PAN with different concentrations of $Mg(NO_3)_2$—(0.2, 0.3, and 0.4 m.m.%). This was interpreted in terms of Hodge et al. [28] criterion, which establishes a correlation between the intensity of the peak and the degree of crystallinity. The increase in salt concentration reveals that as ion concentration in the electrolyte increases, both the fraction of amorphous phase and charge carriers increase simultaneously [29]. From Fig. 1, it has been observed that BPE 92.5PVA:7.5PAN:0.3 m.m.% $Mg(NO_3)_2$ has maximum amorphous nature. The magnitude of amorphous phase usually increases the segmental motion of the polymer by making it more flexible which in turn enhances the conductivity of a polymer electrolyte [30]. Furthermore, beyond the addition of 0.3 m.m.% $(MgNO_3)_2$, the salt gets recrystallizes [31], which reduces the number of charge carriers and the overall ionic conduction of the BPEs which are well consistent with the electrical measurement. The lack of diffraction peaks for $Mg(NO_3)_2$ in the XRD

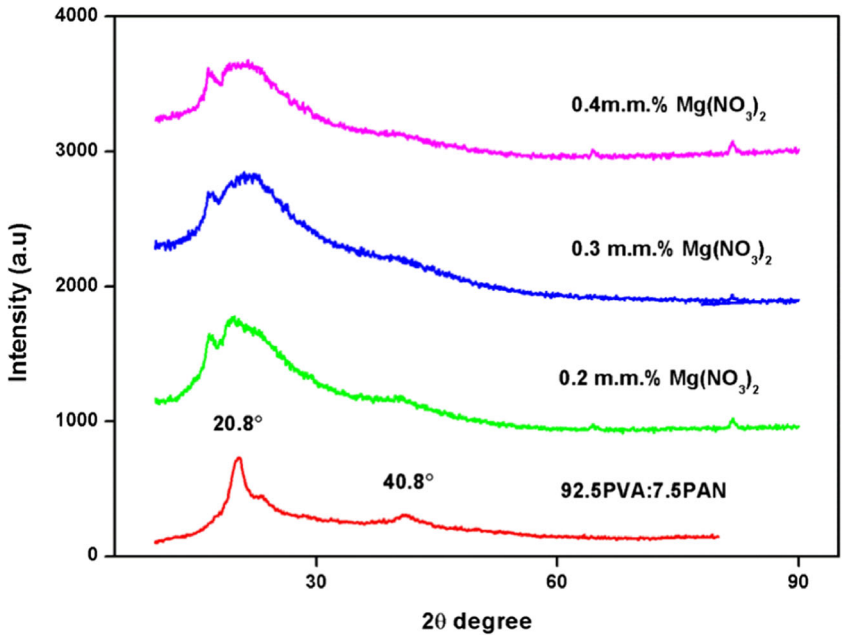

Fig. 1 XRD patterns of pure BPE and 92.5PVA:7.5PAN BPE with different salt concentrations

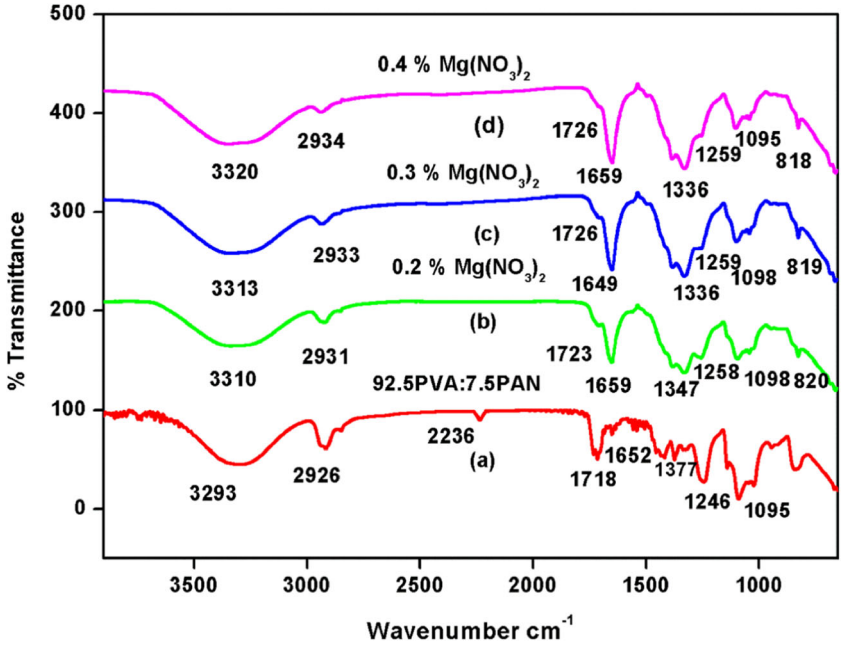

Fig. 2 FTIR pattern of pure 92.5PVA:7.5PAN BPE and BPE with different salt concentrations

pattern of the BPEs indicates the complete dissociation of the salt in the polymer matrix.

Fourier transform infrared (FTIR) spectroscopy analysis

FTIR is a versatile tool to study the interaction of salt with the polymer owing to the changes in the vibrational frequencies of the polymer matrix. Figure 2 predicts the FTIR spectra for pure BPE 92.5PVA:7.5PAN and 92.5PVA:7.5PAN:$Mg(NO_3)_2$ complex of various compositions (0.2, 0.3, and 0.4 m.m.%) in the wavenumber region from 800 to 4000 cm^{-1}.

In Fig. 2, the assignments OH stretching, CH_2 asymmetric stretching, C=C stretching, CH_3 symmetric, C–O–C stretching, and C–C asymmetric have been observed for pure BPE 92.5PVA:7.5PAN at bands 3293, 2926, 1652, 1377, 1240, and 1095 cm^{-1}, respectively. The change in intensity, shape, and position of the bands has been detected when the salt of different concentrations is added. The shifting in vibrational peaks and the corresponding assignments are noted in Table 1.

In the FTIR spectrum of pure BPE (92.5PVA:7.5PAN), a broad absorption band corresponding to H–OH stretching of pure PVA at 3288 cm^{-1} [32] is widened in the salt-added systems. This indicates the coordination between the cation of the salt and hydroxyl group of PVA [33]. The hydroxyl band is shifted toward higher wave number in the complexes which gives strong indication of specific interaction of salt and host polymer 92.5PVA:7.5PAN in the BPEs [34–36]. Since NO^{3-} ion is a nucleophile of negative ion which seeks electron deficient atom which makes an interaction with the carbonyl carbon of the polymer chain. Similarly, Mg^{2+} is an electrophile or positive ion which seeks electron-rich atom to interact, so that it makes a possible interaction with OH^- group

Table 1 FTIR assignments for all the prepared BPEs

92.5PVA:7.5PAN	92.5PVA:7.5PAN:0.2 m.m.% $Mg(NO_3)_2$	92.5PVA:7.5PAN:0.2 m.m.% $Mg(NO_3)_2$	92.5PVA:7.5PAN:0.2 m.m.% $Mg(NO_3)_2$	Assignments
3293	3310	3313	3320	OH stretching
2926	2931	2933	2934	CH_2 asymmetric stretching
2236	–	–	–	C≡N stretching
1718	1723	1726	1726	C=O stretching
1652	1659	1649	1659	C=C stretching
1377	1347	1336	1336	CH_3 asymmetric stretching
1246	1258	1259	1259	C–O–C stretching
1095	1098	1098	1095	C–C asymmetric
	820	819	818	Plane deformation modes of NO^3 ion

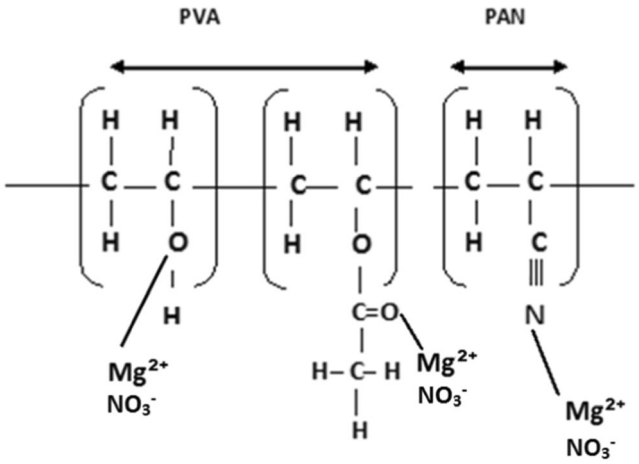

Fig. 3 Possible interaction between blend polymer (PVA:PAN) and $Mg(NO_3)_2$

present in the pure polymer blend. A weak absorption at 2236 cm^{-1} corresponding to C≡N stretching of PAN which is its most characteristic band [37] becomes invisible in the salt-added system which shows the complexation of the salt with the polymer blend. The strong absorption bands at 1347 and 818 cm^{-1} ascribed to CH_3 asymmetric stretching and plane deformation modes of NO^3 ion, respectively [38–40]. All the polymer electrolyte samples (0.2–0.4 m.m.% $Mg(NO_3)_2$) show these characteristic bands of the nitrate group prove the presence of $MgNO_3$ in the electrolyte system. A strong intermolecular interaction between magnesium ion from added salt and oxygen atoms has been observed in salt-added compositions at 1723 cm^{-1} due to the shift in carbonyl group (C=O) stretching vibration. The oxygen atom bonds with magnesium ion from added salts [41]. The shift in stretching modes of the carbonyl bonds observed for the samples with different concentrations (0.2, 0.3, and 0.4 m.m.%) of $Mg(NO_3)_2$ indicates complexation of the polymer.

Figure 3 shows the possible interaction of 92.5PVA:7.5PAN and $Mg(NO_3)_2$. The hydroxyl group, carbonyl group, nitrile group, and NO^{3-} interactions between pure BPE and $Mg(NO_3)_2$ imply that the ions are mobile in the system. As high mobility favors to high ionic conductivity, ion mobility plays a

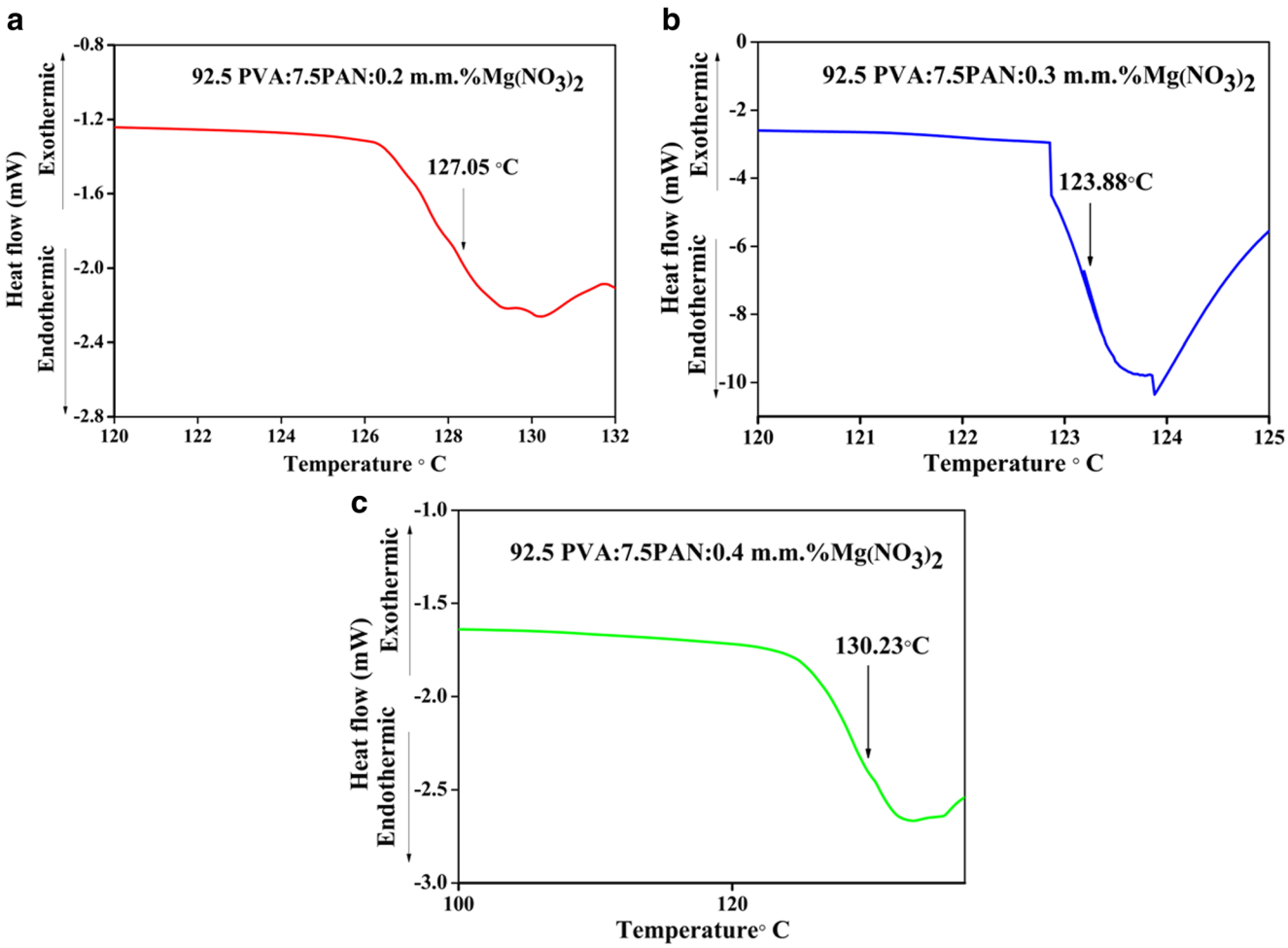

Fig. 4 DSC plot for 92.5PVA:7.5PAN BPE with different salt concentrations (**a, b, c**)

Table 2 Glass transition temperature (T_g) values of 92.5PVA:7.5PAN and $Mg(NO_3)_2$ polymer electrolyte with different salt concentrations

Composition 92.5PVA:7.5PAN:*x* m.m.% $Mg(NO_3)_2$ *x*	Glass transition temperature(°C)
0	136.4° [19]
0.2	127.05
0.3	123.88
0.4	130.23

vital role in an electrolyte system. This confirms that $Mg(NO_3)_2$ has the potential to function as the charge carrier in the system. Under the influence of electric field, a weakly bounded dissociated Mg^{2+} ion proposes a conduction pathway. Through the coordinating site of OH, C=O, and C≡N of host polymer, this Mg^{2+} can hop and the conduction takes place [42]. These results confirm the complexation of host polymer with the salt.

Differential scanning calorimetry

In order to observe the change in glass transition temperature in BPE system, thermal analysis using differential scanning calorimeter (DSC) has been executed. Figure 4 shows the DSC thermogram of 92.5PVA:7.5PAN:*x* $Mg(NO_3)_2$ ($x = 0.2$, 0.3, and 0.4 m.m.%). Sivadevi et al. have previously reported the glass transition temperature for pure blend polymer 92.5PVA:7.5PAN as 136.4 °C [19]. Significantly, the addition of magnesium nitrate can decrease the T_g value of the host polymer. The position of T_g for 92.5PVA:7.5PAN BPE with different concentrations of $Mg(NO_3)_2$ was slightly shifted toward lower temperature. For 0.2 and 0.3 m.m.% of $Mg(NO_3)_2$, the temperature lowers to 127.05 and 123.88 °C, respectively. The decrease in T_g value can pointed to a strong effect of magnesium nitrate on softening of the complexation due to the plasticizing effect of the guest salt on the polymer structure. This is beneficial for the magnesium ion transport in the anhydrous membrane [43]. However for 0.4 m.m.% $Mg(NO_3)_2$ added with 92.5PVA:7.5PAN blend, the T_g was found to be increased to 130.23 °C which may be due to the presence of some undissociated salt in the polymer blend matrix. The glass transition temperature values are listed in Table 2.

Electrochemical impedance spectroscopy analysis

For electrical characterization and determination of σ_{dc} values, impedance spectroscopy is one of the most often used techniques. The impedance analysis of the BPE films was carried out by sandwiching them between two stainless steel plates which act as blocking electrodes for Mg^{2+} ions under an applied electric field. The Cole–Cole plot represented as imaginary (Z") versus real (Z') for 92.5PVA:7.5PAN with different concentrations of $Mg(NO_3)_2$ is shown in Fig. 5. At high frequency, the semicircle is due to the parallel combination of a resistor and a capacitor. The spike in the low frequency is due to electrode/electrolyte contact which can be signified by constant phase element (CPE) connected in series [44] as shown.

In the present system of 92.5PVA:7.5PAN:$Mg(NO_3)_2$, due to the movement of charge carrier in the polymer electrolyte, the capacitive nature of the electrolyte disappears and the resistive component exists which can be proved from the presence of spike alone in the Cole–Cole plot (Fig. 4b). The equivalent circuit was shown along with the Cole–Cole plot in Fig. 4. Using EQ software program developed by Boukamp [45, 46], the electrochemical impedance spectroscopy parameters were obtained and listed in Table 3. Table 3 illustrates the

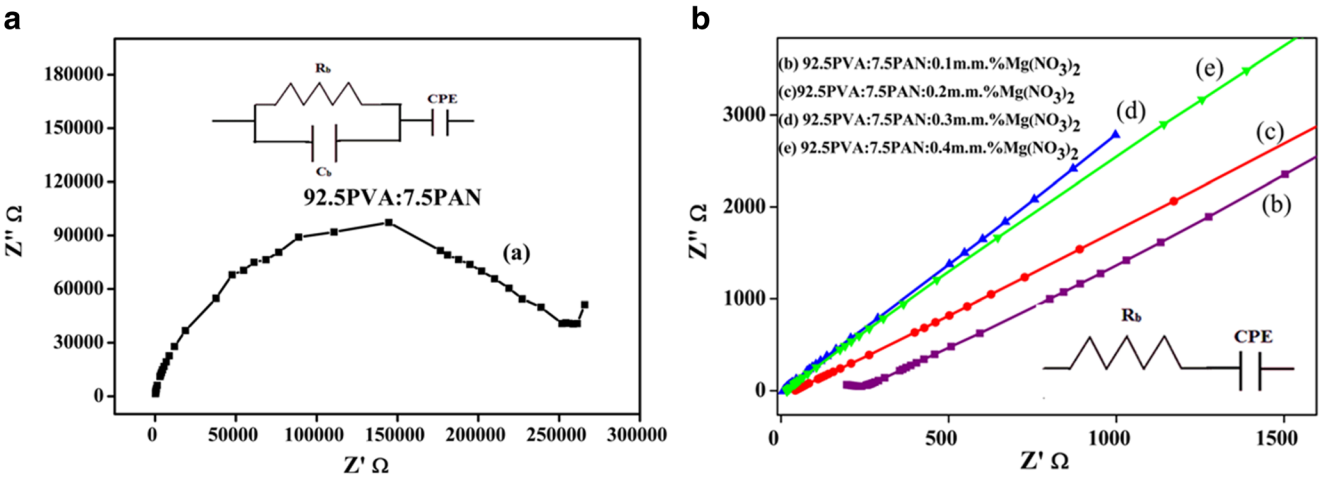

Fig. 5 **a** Cole–Cole plot for pure 92.5PVA:7.5PAN BPE and **b** Cole–Cole plot for BPE with different salt concentrations

Table 3 Ionic conducting data at different temperatures and activation energy for BPEs

Polymer composition 92.5PVA:7.5PAN:*x* wt% $Mg(NO_3)_2$	Ionic conductivity (S cm^{-1})					*R*, Ω	CPE, μF	*n*	Activation energy at room temperature (eV)	Regression value
x	303 K	313 K	323 K	333 K	343 K					
0	1.30×10^{-8}	1.56×10^{-7}	5.03×10^{-7}	3.28×10^{-6}	4.65×10^{-6}	2.3×10^{5}	9.58×10^{-10}	0.85	1.33	0.94
0.1	2.27×10^{-5}	4.78×10^{-5}	7.41×10^{-5}	1.12×10^{-4}	2.27×10^{-4}	2.45×10^{2}	1.68×10^{-6}	0.7	0.49	0.98
0.2	1.64×10^{-4}	1.9×10^{-4}	3.61×10^{-4}	6.54×10^{-4}	1.22×10^{-3}	4.53×10^{1}	3.55×10^{-6}	0.68	0.58	0.99
0.3	1.71×10^{-3}	1.95×10^{-3}	2.13×10^{-3}	3.42×10^{-3}	4.95×10^{-3}	4.58	4.95×10^{-6}	0.77	0.36	0.99
0.4	9.04×10^{-4}	9.77×10^{-4}	1.87×10^{-3}	3.83×10^{-3}	5.4×10^{-3}	1.01×10^{1}	1.13×10^{-5}	0.76	0.55	0.99

resistance value of BPE added with 0.1–0.4 m.m.% $Mg(NO_3)_2$ decreases from 2.45×10^2 to 1.01×10^1 Ω when compared with the pure 92.5PVA:7.5PAN polymer electrolyte whose resistance is 2.3×10^5 Ω.

The CPE for pure blend was obtained as 9.58×10^{-10} F. The $Mg(NO_3)_2$ of 0.05–0.3 m.m.% added with BPE has CPE values in the range of 1.68×10^{-6} F to 1.13×10^{-5} F. The highest conductivity BPE 92.5PVA:7.5PAN:0.3 m.m.% $Mg(NO_3)_2$ has $R_b = 4.58$ Ω and CPE = 4.95×10^{-6} F.

The ionic conductivity of the BPE film depends on the concentration of the conducting species and their mobility. High ionic conductivity around 1.71×10^{-3} S cm^{-1} is obtained for the sample which contains 0.3 wt% of $MgNO_3$ salt in the 92.5PVA:7.5PAN polymer blend. This sample has low bulk resistance (R_b) compared to other samples. It is evident that the low bulk resistance corresponds to high ionic conductivity. The ionic conductivity is calculated using the following equation:

$$\sigma = L/R_b A \tag{1}$$

where L is the thickness of the electrolyte and A is the surface area of the film.

The room temperature ionic conductivity for the prepared BPE's film samples is tabulated in Table 3. From the table, it is observed that the ionic conductivity increases up to 0.3 m.m.wt% $Mg(NO_3)_2$, and further increase in $Mg(NO_3)_2$ concentration beyond 0.3 m.m.wt% results in decrease of ionic conductivity. The decrease in ionic conductivity at high concentration of the salt is due to the ion aggregation in the polymer network [47].

Temperature-dependent conductivity analysis

In the current study, the effect of temperature from room temperature to 70 °C on the ionic conductivity of the prepared BPEs was studied. It is observed in Fig. 6 that as the temperature rises, the conductivity also raises for all complexes and this behavior can be rationalized by recognizing the free volume model [48]. With increase in temperature, the vibrational energy of a segment is far enough to push against the hydrostatic pressure which is imposed by its nearby atoms and create a small void surrounding its own volume in which vibrational motion can occur [49]. This free volume causes the mobility of ions and polymer segments around the polymer chain and hence the conductivity. Hence, the increase in temperature raises the conductivity due to the increased free volume and their respective ionic and segmental mobility. The Arrhenius behavior has been followed for the conductivity temperature plots throughout the range, and the variation in conductivity can be fitted to the relation:

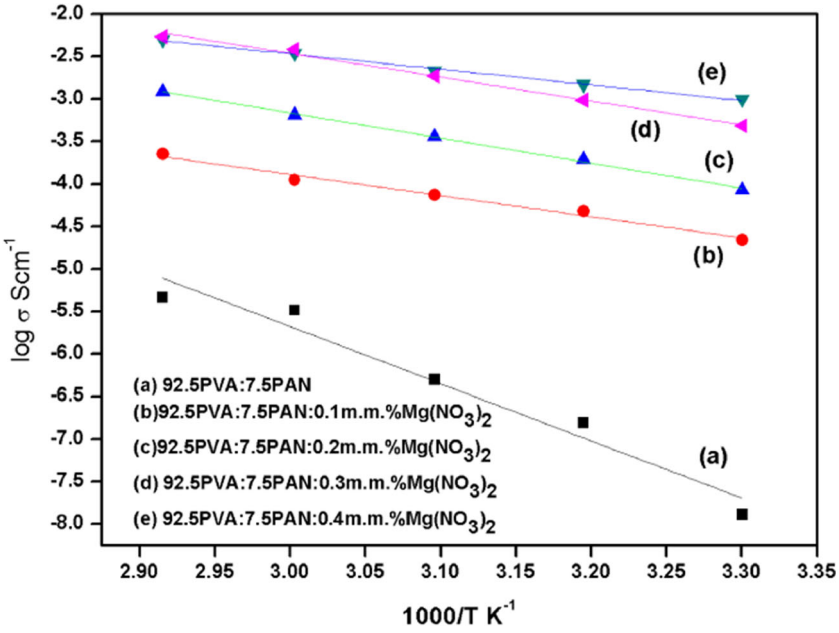

Fig. 6 Temperature dependence ionic conductivity for pure 92.5PVA:7.5PAN BPE and BPE with different salt concentrations

$$\sigma_T = \sigma_0 \exp\left(^{-E_\alpha}/_{KT}\right) \quad (2)$$

where σ, σ_0, E_a, K, and T are the ionic conductivity, pre-exponential factor, activation energy, Boltzmann constant, and absolute temperature, respectively. Figure 5 shows ln(r) versus 1000/T plots for different concentrations of BPEs. A good straight line fit has been obtained for all the 92.5PVA:7.5PAN with $Mg(NO_3)_2$ concentration based on the least squares analysis of the corresponding data. The regression values of all the prepared samples are close to unity, indicating that the temperature-dependent ionic conductivity for this system obeys Arrhenius rule. The activation energy E_a has been calculated for all the BPEs by linear fit of the Arrhenius plot. The outcomes are tabulated in Table 3. The values of activation energy decrease with increasing salt concentration up to 0.3 m.m.% $Mg(NO_3)_2$ which is due to the increase in amorphous nature of the polymer electrolyte which smooths the progress of the ionic motion in the polymer network. Further increase in salt concentration increases the activation energy which may be due to the decrease in amorphous nature.

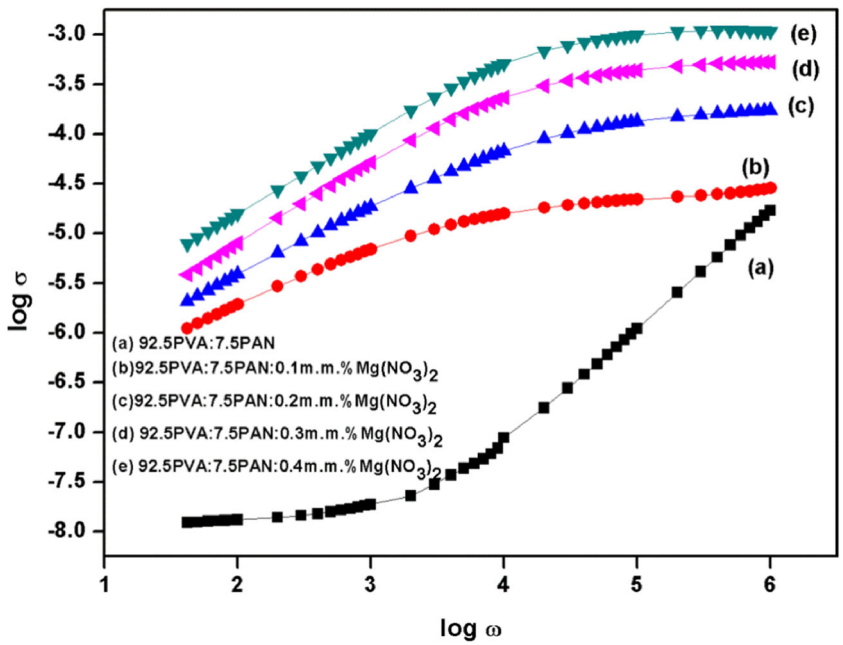

Fig. 7 Conductance spectra for pure 92.5PVA:7.5PAN BPE and BPE with different salt concentrations

Conductance spectrum analysis

In general, the conductance spectra consist of three distinct regions, a low-frequency dispersion region which represents the space charge polarization at the blocking electrodes [50], a mid-frequency plateau region which is caused mainly by the hopping motion of the mobile ions whose extrapolations determine the dc value of the conductivity, and a high-frequency dispersion region corresponding to bulk relaxation phenomenon. Figure 7 shows the conductance spectra of pure BPE 92.5PVA:7.5PAN and BPE added with different concentrations of $Mg(NO_3)_2$. By extrapolating the intermediate plateau region to zero frequency, the d.c. conductivity of the biopolymer membranes has been calculated which was consistent with the conductivity values obtained from Cole–Cole plot. BPE 92.5PVA:7.5PAN:0.3 m.m.% $Mg(NO_3)_2$ has the maximum d.c. conductivity, and further increase in salt concentration decreases the conductivity which may be due to the formation of ion aggregates or to the formation of ion multiplies [48].

Transference number measurement

Wagner's DC polarization technique is one of the fundamental methods to calculate the total ion transport number. In this polarization technique, a SS/BPE/SS cell was polarized by pertaining a step potential of 1 V. The outcoming potentiostatic current was plotted as a function of time. Due to the depletion of ionic species in the electrolyte, the initial total current decreases with time and becomes constant in the fully depleted situation. At the steady state, the cell is polarized and the current flows across the electrolyte interface because of ions. Theoretically, the value of total ion transport number is united. For the highest ion conducting sample 92.5PVA:7.5PAN:0.3 m.m.% $Mg(NO_3)_2$, the total ion transport number calculated using the Eq. (3) is 0.97.

$$t_{ion} = \frac{i_T - i_e}{i_T} \tag{3}$$

Here, i_T is the total current and i_e the residual current. The result shows that the overall conductivity of the sample is predominantly ion and the ion transport value is quite comparable with the theoretical value. This indicates that the electron conduction is quite negligible. It is difficult to evaluate the contribution of charged specie to the total conductivity. Mg^{2+} ion is evaluated using a.c/d.c techniques proposed by Evans et al. [51]. According to this technique, by supplying a constant voltage of $\Delta V = 1.5$ V, the cell (Mg/BPE/Mg) was polarized. At room temperature, the initial and final currents are recorded. Due to (i) passivation layer growth on the electrodes and (ii) concentration gradient formation in the electrolyte, fall of current till steady state was reached. By means of impedance measurements, the cell resistance has been measured before and after polarization. Using EQ software [45, 46], the fitting of the impedance plots has been measured. The impedance plots are shown in Fig. 8a. The impedance of the bulk electrolyte, R_b, has been noted at the intercept of the high-frequency region. At low-frequency region, the total impedance ($R_s = R_b + R_i$) of the cell corresponds to the diameter of the semicircle where R_i represents the resistance of the passivation layer [52].The value of t_{+ion} can be obtained from:

$$t_+ = \frac{I_g(\Delta V - R_0 I_0)}{I_0(\Delta V - R_g I_g)} \tag{4}$$

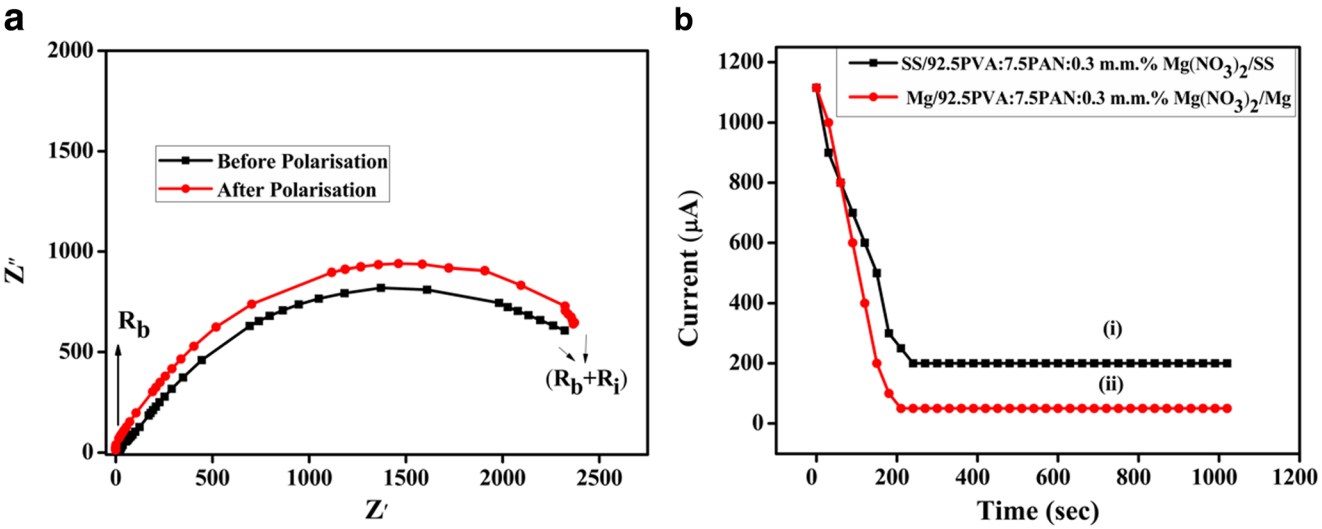

Fig. 8 **a** A.C. complex impedance plot before and after polarization of a typical symmetric Mg/92.5PVA:7.5PAN:0.3 m.m.% $Mg(NO_3)_2$/Mg cell. **b** The D.C. polarization curve of (i) SS/92.5PVA:7.5PAN:0.5 m.m.% $Mg(NO_3)_2$/SS cell and (ii) Mg/92.5PVA:7.5PAN:0.5 m.m.% $Mg(NO_3)_2$ /Mg cell at room temperature

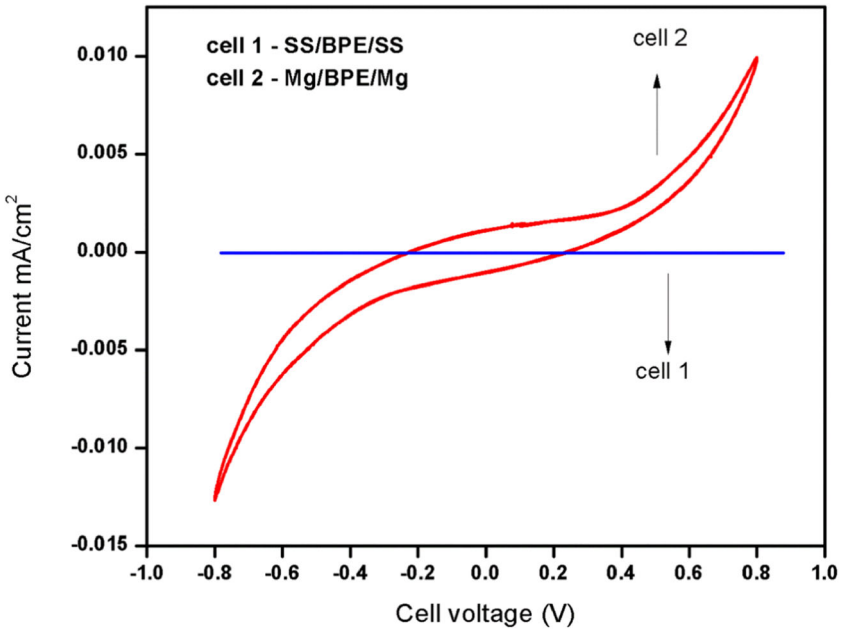

Fig. 9 Cyclic voltammetry of cell 1: SS/ 92.5PVA:7.5PAN:0.3 m.m.% $Mg(NO_3)_2$ /SS and cell 2: Mg/ 92.5PVA:7.5PAN:0.3 m.m.% $Mg(NO_3)_2$/Mg recorded at room temperature at a scan rate of mVs^{-1}

The maximum conducting sample of 92.5PVA:7.5PAN:0.3$MgNO_3$ corresponds to the value of 0.30 as Mg^{2+} ion transport number. These values suggest a significant contribution to the total ionic conduction of the BPE films. Kumar et al. [53] reported that for PMMA-based GPE system using 0.5 g of $Mg(CF_3SO_3)_2$ salt, the transport number for the Mg^{2+} ion is 0.33.

Cyclic voltammetry

Figure 9 represents the cyclic voltammogram for cell 1 and cell 2 containing 92.5PVA:7.5PAN:0.3 m.m.% $Mg(NO_3)_2$ sample sandwiched between two symmetrical magnesium electrodes and two symmetrical SS electrodes done at a scan rate of 5 mV s^{-1}, respectively. For cell 2 (with Mg electrodes), the cathodic and anodic current peaks are distinctly observed. On the other hand, no such features are evident in the case of cell 1 (with SS electrode). This corresponds to the following reversible reaction:

$$Mg^{2+} + 2e^{-} \Leftrightarrow Mg \tag{5}$$

which proves the reversibility of Mg/Mg^{2+} reaction in the solid polymer electrolyte. Further higher magnitude of current in cell 2 than in cell 1 indicates that the cathodic deposition and anodic oxidation of Mg are facile at Mg/BPE interface which confirms Mg^{2+} conduction in BPE. The cathodic and anodic peak potentials are separated by several volts, which is possible with the symmetrical cell with two-electrode geometry without a reference electrode. Similar reports have been reported in the literature [53, 54].

Linear sweep voltammogram

The electrochemical stability of the highest conducting 92.5PVA:7.5PAN:0.3 m.m.% $Mg(NO_3)_2$ polymer electrolyte was determined by linear sweep voltammetry which has been recorded on Mg/BPE/SS cell at a scan rate of 5 mV s^{-1}. By applying voltage to the cell, the current–voltage response curve has been obtained as shown in Fig. 10. The voltage at which the current flows through the cell is considered as the anodic decomposition limit of the polymer electrolyte [55]. From the plot, it is seen that the electrolyte shows the electrochemical stability window of 3.4 V which is a sufficient range for its application in magnesium ion batteries [56]. 3.5 V has

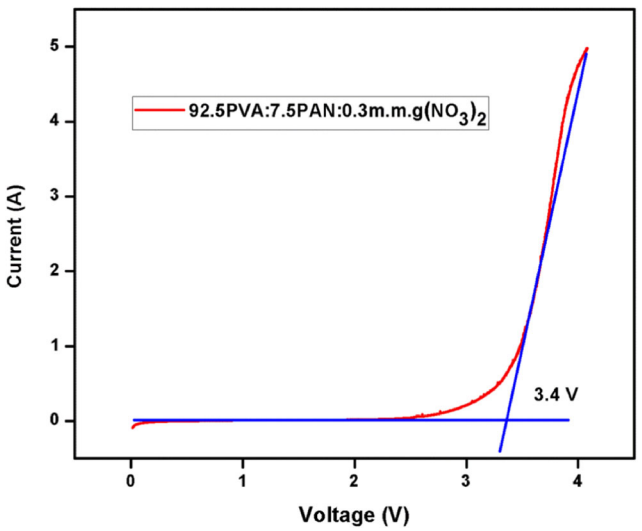

Fig. 10 Linear sweep voltammetry recorded at a scan rate of 1 mV/s at room temperature

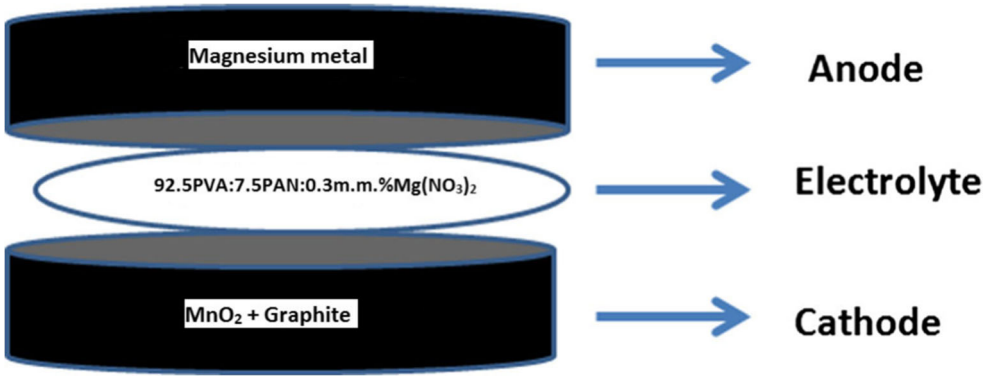

Fig. 11 Battery configuration

been obtained as the stability window by Osman et al., for the electrolyte system SS/PVDF-HFP:20 wt% $(Mg(CF_3SO_3))_2$/Mg [57].

Fabrication of primary Mg primary battery

Preparation of anode–magnesium metal in pellet form was chosen.

Preparation of cathode The required amount of manganese di-oxide (MnO_2) and graphite in the appropriate proportions was grinded together and pressed with 5-ton pressure to form a pellet. Graphite was added to introduce the electronic conductivity.

Mg-ion primary battery has been fabricated using the highest conducting sample 92.5PVA:7.5PAN:0.3 m.m.% $(NO_3)_2$ using the configuration in Fig. 11.

Manjuladevi et al. [58] have given the reactions for the primary Mg-ion battery which are represented as follows:

The oxidation reaction occurs in the anode is,

$$Mg + 2(OH^-) = Mg(OH)_2 + 2e \quad (6)$$

The reduction reaction occurs in cathode is,

$$2MnO_2 + H_2O + 2e = Mn_2O_3 + 2OH^- \quad (7)$$

Overall reaction,

$$Mg + 2MnO_2 + H_2O = Mn_2O_3 + Mg(OH)_2 \quad (8)$$

The molecular structure of PVA in the host polymer PVA:PAN contains hydroxyl group which may be a source of hydroxide ion in Mg-MnO_2 battery. Presence of occluded moisture/H_2O in PVA is also the source of hydroxyl ion. Due to physical forces in microscopic pores non-essential water which is retained, is called as occluded water which occupies space irregularly throughout the solid polymer PVA [59].

The open-circuit voltage of battery constructed with 92.5PVA:7.5PAN:0.3 m.m.% $(NO_3)_2$ polymer electrolyte was initially 2.02 V which slightly reduces to 1.8 V in the first 100 h of assemble. For 1 month, the stable potential of 1.8 V

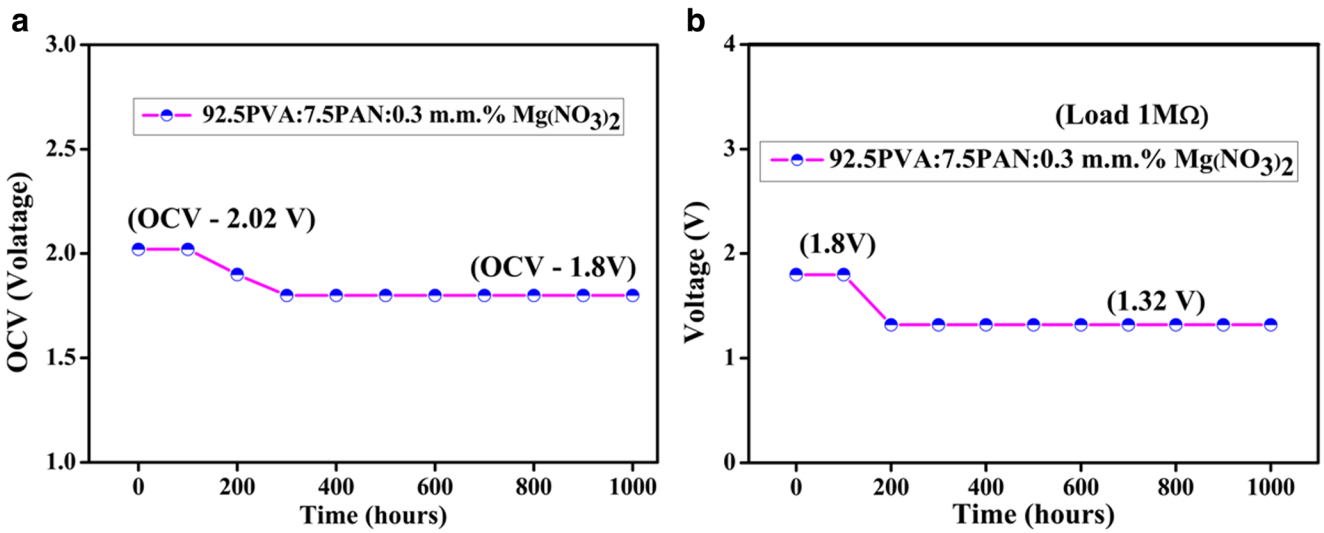

Fig. 12 **a** Open-circuit voltage and **b** discharge characteristics of primary magnesium battery as a function of time for BPE 92.5PVA:7.5PAN:0.3 m.m.% $Mg(NO_3)_2$

Table 4 Cell parameters

Specification of cell parameters	Values of cell parameters
Cell area (cm^2)	1.24
Cell weight (g)	1.3
Effective cell diameter (cm)	1.2
Cell thickness (cm)	0.418
Open circuit voltage (V)	2.02
Cut off potential (h)	800

has been observed. Fig 12a shows the stablized voltage with respect to time. The intermediate drop in the voltage of the cell after fabrication has been observed due to the cell formation reaction. 1.95 V OCV has been reported for PVdF-HFP with 10% of MgO [56].

The discharge characteristics of the battery constructed with 2.5PVA:7.5PAN:0.3 m.m.% $(NO_3)_2$ as electrolyte has been measured with a load of 1 MΩ for 20 days. Discharge behavior of the cell with time was shown in the Fig 12b. Due to the polarization effect at the electrode–electrolyte interface, the initial decrease in potential of the cell occurs [60]. The cell potential discharged at a constant load of 1 MΩ remains constant at 1.32 V for 20 days. The region in which the cell voltage remains constant is called as plateau region. Beyond the plateau region, voltage value of the cell drops again. The OCV and discharge time for the plateau region and other cell parameters are listed in Table 4.

Conclusion

92.5PVA:7.5PAN-based blend polymer electrolyte membranes with $Mg(NO_3)_2$ in different m.m.% (0.1–0.4 m.m.%) have been prepared by solution-casting technique using DMF as solvent. The XRD results revealed that the inclusion of $Mg(NO_3)_2$ alters the crystallinity of the BPE. FTIR analysis confirms the strong complex interaction between 92.5PVA:7.5PAN and $Mg(NO_3)_2$. DSC analysis shows a low T_g value of BPE 92.5PVA:7.5PAN:0.3 m.m.% $Mg(NO_3)_2$. The same membrane offers superior ionic conductivity of 1.71×10^{-3} S/cm at room temperature. The rate of increase of ionic conductivity with temperature exhibits Arrhenius behavior, and the maximum conducting sample exhibits lower activation energy of 0.36 eV. Using Evans et al.'s method, the ionic transference number has been estimated to be 0.30 for the BPE 92.5PVA:7.5PAN:0.3 m.m.% $Mg(NO_3)_2$. The existence of electrochemical equilibrium between the Mg metal and the Mg^{2+} ions in the polymer electrolyte has been proved through cyclic voltammetry analysis. The electrochemical stability window for 92.5PVA:7.5PAN:0.3 m.m.% $Mg(NO_3)_2$ proved that the BPE is suitable to be applied in electrochemical devices. Thus, the optimized membrane 92.5PVA:7.5PAN:0.3 m.m.% $Mg(NO_3)_2$ with high ionic conductivity has been applied for primary magnesium battery which is found to perform with an OCV of 2.02 V.

References

1. Armand M, Tarascon JM (2008) Building better batteries. Nature 451:652–657
2. Crowther O, West AC (2008) Effect of electrolyte composition on lithium dendrite growth. J Electrochem Soc 155:A806–A811
3. Matsui M (2011) Study on electrochemically deposited Mg metal. J Power Sources 196:7048–7055
4. Kim HS, Arthur TS, Allred GD, Zajicek J, Newman JG, Rodnyansky AE, Oliver AG, Boggess WC, Muldoon J (2011) Structure and compatibility of a magnesium electrolyte with a sulphur cathode. Nat Commun 2:427
5. Wu ID, Chang FC (2007) Determination of the interaction within polyester-based solid polymer electrolyte using FTIR spectroscopy. Polymer 48:989–996
6. Papke BL, Ratner MA, Shriver DF (1982) Conformation and ion-transport models for the structure and ionic conductivity in complexes of polyethers with alkali metal salts. J Electrochem Soc 129: 1694–1701
7. Kesavan K, Mathew CM, Rajendran S (2014) Lithium ion conduction and ion-polymer interaction in poly (vinyl pyrrolidone) based electrolytes blended with different plasticizers. Chin Chem Lett 25: 1428–1434
8. Hema M, Tamilselvi P, Hirankumar G (2017) Influences of LiCF3SO3 and TiO2 nanofiller on ionic conductivity and mechanical properties of PVA: PVdF blend polymer electrolyte. Ionics 23: 2707–2714
9. Subramania A, Sundaram NK, Kumar GV, Vasudevan T (2006) New polymer electrolyte based on (PVA–PAN) blend for Li-ion battery applications. Ionics 12:175–178
10. Polu AR, Kumar R, Rhee HW (2015) Magnesium ion conducting solid polymer blend electrolyte based on biodegradable polymers and application in solid-state batteries. Ionics 21:125–132
11. Ramesh S, Winie T, Arof AK (2007) Investigation of mechanical properties of polyvinyl chloride–polyethylene oxide (PVC–PEO) based polymer electrolytes for lithium polymer cells. Eur Polym J 43:1963–1968
12. Rajendran S, Sivakumar P (2008) An investigation of PVdF/PVC-based blend electrolytes with EC/PC as plasticizers in lithium battery applications. Phys B Condens Matter 403:509–516
13. Subramania A, Sundaram NK, Kumar GV (2006) Structural and electrochemical properties of micro-porous polymer blend electrolytes based on PVdF-co-HFP-PAN for Li-ion battery applications. J Power Sources 153:177–182
14. Mohamad AA, Mohamed NS, Yahya MZA, Othman R, Ramesh S, Alias Y, Arof AK (2003) Ionic conductivity studies of poly (vinyl alcohol) alkaline solid polymer electrolyte and its use in nickel–zinc cells. Solid State Ionics 156:171–177
15. Kadir MFZ, Majid SR, Arof AK (2010) Plasticized chitosan–PVA blend polymer electrolyte based proton battery. Electrochim Acta 55:1475–1482
16. Yuan HK, Ren J, Ma XH, Xu ZL (2011) Dehydration of ethyl acetate aqueous solution by pervaporation using PVA/PAN hollow fiber composite membrane. Desalination 280:252–258
17. Kim DH, Na SK, Park JS, Yoon KJ, Ihm DW (2002) Studies on the preparation of hydrolyzed starch-g-PAN (HSPAN)/PVA blend films—effect of the reaction with epichlorohydrin. Eur Polym J 38:1199–1204

18. Ma XH, Xu ZL, Liu Y, Sun D (2010) Preparation and characterization of PFSA–PVA–SiO 2/PVA/PAN difunctional hollow fiber composite membranes. J Membr Sci 360:315–322
19. Sivadevi S, Selvasekarapandian S, Karthikeyan S, Sanjeeviraja C, Nithya H, Iwai Y, Kawamura J (2015) Proton-conducting polymer electrolyte based on PVA-PAN blend doped with ammonium thiocyanate. Ionics 21:1017–1029
20. Sivadevi S, Selvasekarapandian S, Karthikeyan S, Vijaya N, Kingslin Mary Genova F, Sanjeeviraja C (2013) Structural and AC impedance analysis of blend polymer electrolyte based on PVA and PAN. Int J Sci Res. https://doi.org/10.15373/22778179
21. Sivadevi S, Selvasekarap S, Karthikeyan S, Vijaya N, Kingslin F, Genova M et al (2013) Proton-conducting polymer electrolyte based on PVA-PAN blend polymer Doped with NH_4NO_3. Int J Electroactive Mater 1:64–70
22. Genova FKM, Selvasekarapandian S, Karthikeyan S, Vijaya N, Pradeepa R, Sivadevi S (2015) Study on blend polymer (PVA-PAN) doped with lithium bromide. Polymer Science Series A 57: 851–862
23. Francis KMG, Subramanian S, Shunmugavel K, Naranappa V, Pandian SSM, Nadar SC (2016) Lithium ion-conducting blend polymer electrolyte based on PVA–PAN doped with lithium nitrate. Polym-Plast Technol Eng 55:25–35
24. Kumar GG, Munichandraiah N (2001) Solid-state rechargeable magnesium cell with poly (vinylidenefluoride)–magnesium triflate gel polymer electrolyte. J Power Sources 102:46–54
25. Kumar GG, Munichandraiah N (2002) Poly (methylmethacrylate)—magnesium triflate gel polymer electrolyte for solid state magnesium battery application. Electrochim Acta 47:1013–1022
26. Osman Z, Zainol NH, Samin SM, Chong WG, Isa KM, Othman L et al (2014) Electrochemical impedance spectroscopy studies of magnesium-based polymethylmethacrylate gel polymer electroytes. Electrochimica Acta 131:148–153
27. Kim JH, Lee YM (2001) Gas permeation properties of poly (amide-6-b-ethylene oxide)–silica hybrid membranes. J Membr Sci 193(2): 209–225
28. Hodge RM, Edward GH, Simon GP (1996) Water absorption and states of water in semicrystalline poly (vinyl alcohol) films. Polymer 37:1371–1376
29. Aji MP, Masturi M, Bijaksana S, Khairurrijal K, Abdullah M (2012) A general formula for ion concentration-dependent electrical conductivities in polymer electrolytes. Am J Appl Sci 9(6):946–954
30. Ravi M, Song S, Wang J, Wang T, Nadimicherla R (2016) Ionic liquid incorporated biodegradable gel polymer electrolyte for lithium ion battery applications. J Mater Sci Mater Electron 27:1370–1377
31. Reddy MJ, Chu PP (2002) Effect of Mg 2+ on PEO morphology and conductivity. Solid State Ionics 149(1):115–123
32. Fattoum A, Arous M, Pedicini R, Carbone A, Charnay C (2015) Conductivity and dielectric relaxation in crosslinked PVA by oxalic and citric acids. Polymer Science Series A 57:321–329
33. Pandey GP, Agrawal RC, Hashmi J (2011) Magnesium ion-conducting gel polymer electrolytes dispersed with fumed silica for rechargeable magnesium battery application. Solid State Electrochem 15:2253–2264
34. Rajendran S, Sivakumar M, Subadevi R (2003) Effect of salt concentration in poly (vinyl alcohol)-based solid polymer electrolytes. J Power Sources 124(1):225–230
35. Abdelrazek EM, Elashmawi IS, Labeeb S (2010) Chitosan filler effects on the experimental characterization, spectroscopic investigation and thermal studies of PVA/PVP blend films. Phys B Condens Matter 405:2021–2027
36. Pu H, Huang P (2006) Studies on transparent and solid proton conductors based on NH 4 H 2 PO 4 doped poly (vinyl alcohol). Mater Lett 60:1724–1727
37. Coleman MM, Petcavich RJ (1978) Fourier transform infrared studies on the thermal degradation of polyacrylonitrile. J Polym Sci B Polym Phys 16:821–832
38. Wahab A, Mahiuddin S (2008) Density, ultrasonic velocity, electrical conductivity, viscosity, and Raman spectra of methanolic Mg (ClO4) 2, Mg (NO3) 2, and Mg (OAc) 2 solutions. J Chem Eng Data 54(2):436–443
39. Wahab A, Mahiuddin S, Hefter G, Kunz W, Minofar B, Jungwirth P (2005) Ultrasonic velocities, densities, viscosities, electrical conductivities, Raman spectra, and molecular dynamics simulations of aqueous solutions of Mg (OAc) 2 and Mg (NO3) 2: Hofmeister effects and ion pair formation. J Phys Chem B 109(50):24108–24120
40. Béléké AB, Mizuhata M, Kajinami A, Deki S (2003) Diffuse reflectance FT-IR spectroscopic study of interactions of α-Al 2 O 3/ molten alkali nitrate coexisting systems. J Colloid Interface Sci 268: 413–424
41. Su'ait MS, Ahmad A, Badri KH, Mohamed NS, Rahman MYA, Ricardo CA, Scardi P (2014) The potential of polyurethane bio-based solid polymer electrolyte for photoelectrochemical cell application. Int J Hydrog Energy 39:3005–3017
42. Reddy MJ, Chu PP (2002) Ion pair formation and its effect in PEO: Mg solid polymer electrolyte system. J Power Sources 109:340–346
43. Polu AR, Kumar R (2013) Preparation and characterization of pva based solid polymer electrolytes for electrochemical cell applications. Chin J Polym Sci 31:641–648
44. Sengwa RJ, Dhatarwal P, Choudhary S (2014) Role of preparation methods on the structural and dielectric properties of plasticized polymer blend electrolytes: correlation between ionic conductivity and dielectric parameters. Electrochim Acta 142:359–370
45. Boukamp BA (1986) A nonlinear least squares fit procedure for analysis of immittance data of electrochemical systems. Solid State Ionics 20(1):31–44
46. Boukamp BA (1986) A package for impedance/admittance data analysis. Solid State Ionics 18:136–140
47. Ramya CS, Selvasekarapandian S, Savitha T, Hirankumar G, Baskaran R, Bhuvaneswari MS, Angelo PC (2006) Conductivity and thermal behavior of proton conducting polymer electrolyte based on poly (N-vinyl pyrrolidone). Eur Polym J 42(10):2672–2677
48. Miyamoto T, Shibayama K (1973) Free-volume model for ionic conductivity in polymers. J Appl Phys 44(12):5372–5376
49. MacCallum JR, Vincent CA (eds.) (1989) Polymer electrolyte reviews vol. 2. Springer Science & Business Media, Berlin
50. Teeters D, Neuman RG, Tate BD (1996) The concentration behavior of lithium triflate at the surface of polymer electrolyte materials. Solid State Ionics 85(1–4):239–245
51. Evans J, Vincent CA, Bruce PG (1987) Electrochemical measurement of transference numbers in polymer electrolytes. Polymer 28(13):2324–2328
52. Kumar Y, Hashmi SA, Pandey GP (2011) Ionic liquid mediated magnesium ion conduction in poly (ethylene oxide) based polymer electrolyte. Electrochim Acta 56(11):3864–3873
53. Kumar GG, Munichandraiah N (2002) Poly (methylmethacrylate)—magnesium triflate gel polymer electrolyte for solid state magnesium battery application. Electrochim Acta 47(7):1013–1022
54. Pandey GP, Hashmi SA (2009) Experimental investigations of an ionic-liquid-based, magnesium ion conducting, polymer gel electrolyte. J Power Sources 187(2):627–634
55. TianKhoon L, Ataollahi N, Hassan NH, Ahmad A (2016) Studies of porous solid polymeric electrolytes based on poly (vinylidene

fluoride) and poly (methyl methacrylate) grafted natural rubber for applications in electrochemical devices. J Solid State Electrochem 20(1):203–213
56. Pandey GP, Agrawal RC, Hashmi SA (2011) Performance studies on composite gel polymer electrolytes for rechargeable magnesium battery application. J Phys Chem Solids 72(12):1408–1413
57. Rosdi A, Zainol NH, Osman Z (2016) In: AIP Conference Proceedings, vol. 1711 no. 1, AIP Publishing, p 050003
58. Manjuladevi R, Thamilselvan M, Selvasekarapandian S, Mangalam R, Premalatha M, Monisha S (2017) Mg-ion conducting blend polymer electrolyte based on poly (vinyl alcohol)-poly (acrylonitrile) with magnesium perchlorate. Solid State Ionics 308:90–100
59. Manjuladevi R, Thamilselvan M, Selvasekarapandian S, Selvin PC, Mangalam R, Monisha S (2017) Preparation and characterization of blend polymer electrolyte film based on poly (vinyl alcohol)-poly (acrylonitrile)/MgCl2 for energy storage devices. Ionics. https://doi.org/10.1007/s11581-017-2273-9
60. Reddy CVS, Sharma AK, Rao VN (2003) Conductivity and discharge characteristics of polyblend (PVP+ PVA+ KIO 3) electrolyte. J Power Sources 114(2):338–345